Quantitative study of the enhancement of the thermal conductivity of AlN ceramics by nanoscale processing

2009 J. Phys.: Condens. Matter 21 174207

(http://iopscience.iop.org/0953-8984/21/17/174207)

J. Phys.: Condens. Matter **21** (2009) 174207 (5pp) doi:10.1088/0953-8984/21/17/174207

Quantitative study of the enhancement of the thermal conductivity of AlN ceramics by nanoscale processing

A AlShaikhi and G P Srivastava

School of Physics, University of Exeter, Stocker Road, Exeter EX4 4QL, UK

Received 8 September 2008
Published 1 April 2009
Online at stacks.iop.org/JPhysCM/21/174207

Abstract

We have theoretically studied and quantitatively analysed the enhancement of the thermal conductivity of AlN *microceramics* (i.e. commercially available powder) by the insertion of AlN nanosized particles of high-specific surface area, and of Y_2O_3 and CaO as sintering additives. We have also studied the enhancement of the thermal conductivity of AlN *nanoceramics* by using Y_2O_3 as the sintering additive. Thermal conductivity calculations have been carried out by applying the Callaway theory in its full form and by incorporating a detailed and accurate account of three-phonon processes. The role of densification of the AlN ceramic samples in enhancing the thermal conductivity has been quantified at low, intermediate and high temperatures. In addition to explaining the experimentally observed room-temperature conductivity results, the conductivity variation has been predicted over a large temperature range.

(Some figures in this article are in colour only in the electronic version)

1. Introduction

Ever since the potential applications of aluminium nitride (AlN) in microelectronics were realized in the mid-1980s, research on this material has been growing continuously. AlN is a non-toxic material which possesses an excellent combination of properties. It is a hard material with high thermal conductivity, high electrical resistivity, low thermal expansion coefficient (close to that of silicon), low dielectric constant, low loss tangent and wide-direct band gap of 6.2 eV at room temperature [1–3]. These useful properties have made AlN an excellent candidate for substrate material for microelectronics, e.g. for electronic packaging or other temperature-sensitive electronic components. In such applications AlN is required, mainly, to dissipate heat and, thus, the interest in this material is mainly due to its '*high thermal conductivity*' character [4]. The room-temperature thermal conductivity of a pure single-crystal AlN was predicted to be 319 W m^{-1} K^{-1} [5].

The high production cost of growing single-crystal AlN has hindered its usage for commercial-scale technology. Progress has been made in producing AlN ceramics at lower costs. However, AlN ceramic samples contain a large number of impurities (mainly oxygen), point defects (vacancies, small vacancy–impurity complexes, and interstitials) and extended or microstructural defects (large vacancy–impurity complexes, dislocations, stacking faults). Consequently, measured thermal conductivity values for ceramic samples are much lower than the prediction for single-crystal samples (typically in the range 30–272 W m^{-1} K^{-1} [6, 8]). Achieving thermal conductivity κ values of larger than 200 W m^{-1} K^{-1} for ceramic samples requires a careful control of both (i) powder preparation conditions and (ii) the sintering process [6, 7]. Within these two general considerations, several key parameters have been identified for controlling/improving the thermal conductivity of AlN ceramics [8–11]: (a) amount of grain boundary phase, (b) conductivity of grains, (c) additives and (d) sintering time, temperature and pressure. These key parameters do not normally influence the goal of achieving conductivity improvement independently, but act in a co-operative manner. For example, sintering under high pressure at high temperatures in the presence of additives is found to be most effective.

It is almost impossible to eliminate impurity contamination in AlN because of its large affinity for oxygen. However, reducing the level of oxygen impurities in AlN ceramic samples is possible through the use of sintering aids, such as Y_2O_3 or CaO, which form a liquid phase and improve the thermal

conduction process [10]. It has been realized by several researchers that there is an optimum amount of such additives that helps in reducing the concentration of oxygen in AlN ceramics when used as a sintering aid. Hsieh *et al* [12] have suggested that higher than the optimum amount of Y_2O_3 forms thicker secondary phases between the grain boundaries, which act as thermal barriers and consequently cause a decrease in the thermal conductivity.

Densification of AlN ceramic is another important factor to enhance its thermal conductivity. Because of the strong covalent bonding nature of AlN, it difficult to densify ceramic samples during the normal sintering process. Usually hot-pressing or pressureless sintering at high temperature with sintering aids are required for achieving densification. Recently, two nanoscale processing approaches which are effective in enhancing densification and thermal conductivity of AlN ceramics at lower temperatures and low (or zero) pressure have been experimentally established [13, 14]. The first approach involves adding AlN nanosized particles to the mixture of Y_2O_3, CaO and commercially available ceramic powder [13], while the second approach involves adding Y_2O_3 to AlN nanocrystalline ceramic [14]. However, the resultant enhanced thermal conductivity of AlN ceramics has been measured experimentally only at room temperature.

In this work, we present a quantitative estimate of the role of densification of AlN ceramics in enhancing its thermal conductivity by using the two nanoscale processing methods mentioned above. We provide theoretical support to the idea that densification helps additives to play a more effective role in purifying AlN ceramic (i.e. reduction in the amount of impurities) at lower pressureless sintering temperature. The results of this work go beyond explaining the experimentally observed room-temperature conductivity results by predicting the variation of the conductivity over a large temperature range.

2. Theory

One of the most widely used theories of lattice thermal conductivity is the model relaxation-time formulation by Callaway [15]. Within Debye's isotropic continuum model for phonon dispersion relations, Callaway's expression for thermal conductivity can be written as [16]

$$K_c = \frac{\hbar^2 q_D^5}{6\pi^2 k_B T^2}\left[\sum_s c_s^4 \int_0^1 dx\, x^4 \tau \bar{n}(\bar{n}+1) + \frac{\{\sum_s c_s^2 \int_0^1 dx\, x^4 \tau \tau_N^{-1} \bar{n}(\bar{n}+1)\}^2}{\sum_s \int_0^1 dx\, x^4 \tau_N^{-1}(1-\tau\tau_N^{-1})\bar{n}(\bar{n}+1)}\right], \\ = K_D + K_{N-\text{drift}}, \quad (1)$$

where s is the polarization index, q_D is the Debye radius, $x = q/q_D$ is the reduced wavenumber, $\bar{n}$ is the Bose–Einstein phonon equilibrium distribution function and $\tau \equiv \tau(\mathbf{q}, s)$ is relaxation time for a phonon in mode $\mathbf{q}s$. The first term, K_D, is the Debye term and provides the conductivity contribution within the so-called 'single-mode relaxation-time' theory. The second term, $K_{N-\text{drift}}$, also called the N-drift term, provides an additive correction to the 'single-mode relaxation-time' theory. This arises when momentum conserving phonon–phonon normal (N) processes are added together with momentum non-conserving Umklapp (U) and other resistive processes. It has been shown in the past [17–19] that $K_{N-\text{drift}}$ is not only a correction over the Debye term K_D, but is essential in determining the correct magnitude as well as the temperature variation of the conductivity.

The main sources of phonon scattering in AlN ceramics are: grain size, isotopic impurities, other impurities/defects, and anharmonicity. Following Matthiessen's rule, the total phonon relaxation rate can be expressed as $\tau^{-1} = \tau_{bs}^{-1} + \tau_{md}^{-1} + \tau_{GB}^{-1} + \tau_{3ph}^{-1}$, with the contributions arising from boundary, point defects, grain boundary and three-phonon processes, respectively. The boundary scattering rate is simply expressed as $\tau_{bs}^{-1} = c_s/L$, where c_s is the phonon speed for polarization s and L is the phonon mean free path determined by the average grain size.

The most relevant impurities/defects in AlN originate from the presence of oxygen. Oxygen-related defects in AlN occur in two distinct forms: as point defects and as small aggregates (or clusters) [20]. Such impurities and defects evolve as a function of oxygen concentration. It is believed that oxygen incorporation generates Al vacancies and oxygen substitution at N sites. For example, it has been proposed that for oxygen concentration below 0.75 at.%, every Al vacancy (V_{Al}) is surrounded by three substituted oxygen atoms (O_N) and above 0.75 at.% a V_{Al} is surrounded by an octahedrally bonded O_N configuration [20]. Al vacancies (V_{Al}, oxygen substitution at N sites (O_N) and the Al–oxygen complexes (V_{Al}–O_N), act as scattering centres for phonons, the heat carriers in AlN. We estimate that the size of the defect complex for the oxygen concentrations in the samples studied by Qiu *et al* [13] and in the samples studied by Panchula and Ying [14] are smaller than the wavelength of the dominant phonon mode in AlN. With this in mind, we apply the Rayleigh scattering formula [16] for phonon scattering by oxygen-related defects in point and small-cluster forms. The Rayleigh formula for phonon scattering from point (or small size) defects can be expressed as [16]

$$\tau_{md}^{-1} = A\omega^4, \quad (2)$$

where ω is the phonon frequency and the coefficient A depends on the nature of the impurity/defect. For a single crystal with only isotopic impurities, A can be expressed as [16] $A = \frac{\Omega\Gamma}{4\pi\bar{c}^3}$, where $\bar{c}$ is the average phonon speed and $\Gamma = \sum_i f_i \frac{\delta M_i}{\bar{M}}$ is the mass-defect scattering parameter, f_i is the percentage of ith isotope present in the crystal, $\bar{M}$ is the average atomic mass of all the isotopes present in the crystal and $\delta M_i = |M_i - \bar{M}|$, with M_i being the mass of ith isotope. However, there is lack of information regarding the precise nature and concentration of defects in AlN ceramics with and without the incorporation of the additive Y_2O_3. With this in mind, in this work we use the Rayleigh scattering formula in equation (2) with A considered as an adjustable parameter.

Phonon scattering by a grain boundary can be expressed as [21]

$$\tau_{GB}^{-1} = B_{GB}\omega^2, \quad (3)$$

if the spacing between dislocations is much smaller than the phonon wavelength, and as [21]

$$\tau_{GB}^{-1} = B_{GB}\omega^n, \quad (4)$$

Table 1. Parameters used in this work.

Sample	ρ (g cm^{-3})	L (μm)	A (10^{-46} s^3)	B_{GB} (10^{-17} s)	Other parameters
AYC2	2.78	0.9	475	1.8	$c_{TA} = 4.85$ km s^{-1}
AYC2-nano	3.28	2	39	1.7	$c_{LA} = 8.97$ km s^{-1}
Nano-AlN, no additives	3.26	2	15	1.7	$q_D = 1.9 \times 10^{10}$ m^{-1}
Nano-AlN 4 wt% Y_2O_3	3.3	5	3	1.65	

with $0 \leqslant n \leqslant 1$ if the spacing between dislocations is larger than the phonon wavelength, where B_{GB} is the grain boundary coefficient. However, for the systems under study in this work, the minimum phonon wavelength is larger than grain sizes, so the phonon relaxation rate due to grain boundary scattering has been calculated using equation (3).

The most important anharmonic phonon interaction involves three-phonon processes. Following Srivastava's scheme [16], the three-phonon relaxation time for a phonon with wavevector $\mathbf{q}$ and polarization s is expressed as a compound function of frequency and temperature in the form

$$\tau_{3ph}^{-1} = \frac{\hbar q_D^5 \gamma^2}{4\pi\rho\bar{c}^2} \sum_{s's''\epsilon} c_s c_{s'} \times \left[\int dx' x'^2 x''_+ \{1 - \epsilon + \epsilon(Cx + Dx')\} \frac{\bar{n}_{\mathbf{q}'s'}(\bar{n}''_+ + 1)}{(\bar{n}_{\mathbf{q}s} + 1)} + \frac{1}{2} \int dx' x'^2 x''_- \{1 - \epsilon + \epsilon(Cx - Dx')\} \frac{\bar{n}_{\mathbf{q}'s'} \bar{n}''_-}{\bar{n}_{\mathbf{q}s}} \right], \quad (5)$$

where $\omega = qc_s$, $x' = q'/q_D$, $x''_\pm = Cx \pm Dx'$ and $\bar{n}''_\pm = \bar{n}(x''_\pm)$, $C = c_s/c''_s$, $D = c'_s/c''_s$ and $\epsilon = 1(-1)$ for N(U) processes. The first and the second terms in the above equation are contributed by class 1 events (carrier phonon jointly annihilating with another phonon to produce a third phonon) and class 2 events (carrier phonon decaying into two phonons) respectively. Integration limits for the variable x' for allowed combinations of the polarization branch s, s' and s'' are presented in [16]. The Grüneisen constant γ is a measure of crystal anharmonicity. Although γ is a temperature dependent constant [22], a mode-averaged value of 0.5 has been used in this work.

3. Results

As mentioned in introduction, in this work we present a quantitative estimate of the role of material densification in enhancing the thermal conductivity of AlN ceramic samples by using two nanoscale processing methods. Table 1 lists all the parameters used in our work. Before we discuss our results for these samples, it is worth mentioning here that the theory used in this work has been successful in reproducing experimentally measured thermal conductivity results for a number of AlN samples (single crystals and ceramics) at low, intermediate and high temperatures [23]. Figure 1 shows the level of agreement between theory and experiment for two selected examples, a single-crystal sample [5] and a ceramic sample [6]. We, thus, are confident of the results predicted in the entire temperature range for the samples studied in this work.

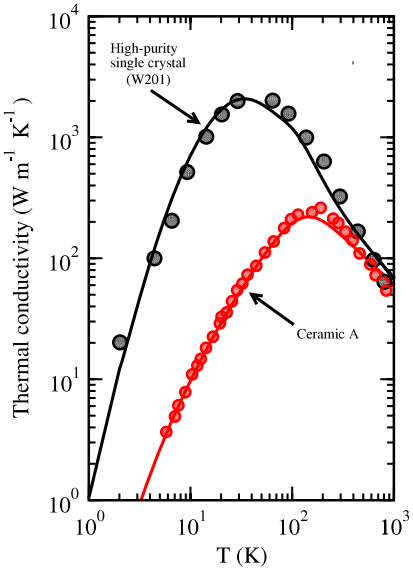

Figure 1. Thermal conductivity of AlN: high-purity single crystal (W201) and ceramic A. The lines show the calculated results and the symbols show the measurements reported in [5] and [6].

3.1. Microcrystalline AlN with additives and nanoparticle dopants

We considered the AYC2 and AYC2-nano samples of AlN presented in the work by Qiu *et al* [13]. Both these samples contained the same amount of Y_2O_3 and CaO additives (3.53 mass% and 2.0 mass%, respectively) as sintering aids. The AYC2-nano sample contained a small amount of 1.89 mass% of AlN nanosized particles (<100 nm) of specific surface area of 70 cm^2 g^{-1} as dopants. The addition of the nanoparticle dopants caused the green density of the sample to increase by a small amount, from 1.87 g cm^{-3} for AYC2 to 1.91 g cm^{-3} for AYC2-nano. After sintering at 1600 °C for 6 h, the reported density of the AYC2 sample increased by 48.7% to 2.78 g cm^{-3} and the density of the AYC2-nano sample increased by 71.7% to 3.28 g cm^{-3}. The density of sintered AYC2-nano is 18% higher than the density of sintered AYC2.

In order to quantify the enhancement in the thermal conductivity of the sample AYC2 due to the addition of nanosized particles over a large temperature range, we started by matching our theoretical thermal conductivity results at room temperature with the experimentally measured results reported in [13] for the sintered samples AYC2 and AYC2-nano. For this purpose we used the material densities and grain boundary sizes reported in [13] and adjusted the impurity/defect scattering parameter A and the grain boundary

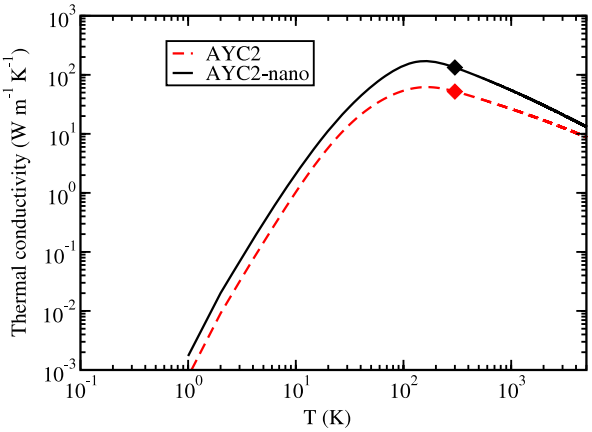

Figure 2. Thermal conductivity of the AlN ceramic samples AYC2 and AYC2-nano. The lines show the calculated results and the symbols show the room-temperature measurements reported in [13].

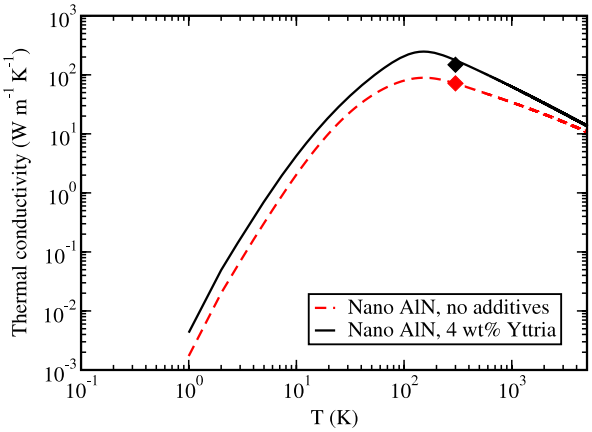

Figure 3. Thermal conductivity of the samples 'Nano-AlN, no additive' and 'Nano-AlN, 4 wt% Y_2O_3' as described in the text and table 1. The lines show the calculated results and the symbols show the room-temperature measurements reported in [14].

scattering parameter B_{GB} to the values shown in table 1. Using these fitted parameters, calculations were extended to several other temperatures. The results of the predicted thermal conductivity for the two samples in low, intermediate and high temperature ranges are shown in figure 2.

In the low temperature regime, the increase in thermal conductivity of AYC2-nano over AYC2 is mainly attributed to the increase in the average grain size due to the addition of nanodopants. At 10 K, the thermal conductivity increases by 100%. The change in density has no effect on thermal conductivity at low temperatures. The maximum increase in thermal conductivity due to the addition of the nanosized particles occurs in the intermediate temperature regime (100–500 K). In this temperature range, the thermal conductivity is heavily influenced by impurity levels, and grain size has no effect. For example, at room temperature the increase in the conductivity is about 155%. Only 7% of this increase is due to the increase in the density, while the rest is primarily due to the reduction in the impurity/defect concentration. This clearly suggests that in addition to increasing the material density, the incorporation of AlN nanosized dopants has facilitated a reduction of impurity/defect concentration caused by the presence of other dopants (namely, CaO and Y_2O_3). The maximum thermal conductivities for AYC2 and AYC2-nano samples are 70 and 170 W m^{-1} K^{-1}, respectively. The position of the peak of the thermal conductivity is shifted slightly from 164 K for the AYC2 sample to 160 K for the AYC2-nano sample. (Such a shift can also be seen in figure 1 where the more oxygen-contaminated ceramic sample has a thermal conductivity peak located at higher temperature than the temperature at which the conductivity of the high-purity single-crystal peaks.) At higher temperatures, typically above 500 K, the role of density becomes more noticeable. This is understandable since three-phonon interaction processes begin to take over control of thermal conductivity and the role of impurity scattering becomes progressively less important. At 1000 K the total increase in the conductivity is 88%, of which 10% is contributed by the increase in the density.

3.2. Nanocrystalline AlN with additives

We consider two samples prepared and studied in the work by Panchula and Ying [14]. The first sample is an additive-free nanocrystalline AlN, referred to as 'Nano-AlN, no additive'. The second sample is a 4 wt% Y_2O_3-doped nanocrystalline AlN, referred to as 'Nano-AlN, 4 wt% Y_2O_3. The densities of these two samples, after pressurelessly sintering at 1900 °C for 2 h, are given in table 1. Panchula and Ying [14] have stated that the final grain size of their additive-free nanocrystalline sample was 2–3 μm. In this work we have considered the average grain size of that sample as 2 μm. There is no experimentally reported value for the average grain size of the second sample, so we made a guess based on a realistic consideration. As sintering at high temperatures in the presence of additives normally results in larger grain sizes, the average grain size in the second sample must be larger than that in the first sample. In order to make a firm judgement, we note that the results presented in another work by Jackson *et al* [10] found that the average grain size of their AlN ceramic sample increased from about 2 μm to about 5 μm after sintering for 100 min with 4.9 wt% of Y_2O_3 as sintering additive. With this in mind, we fixed the average grain size of the second sample as 5 μm. Following the procedure described in the previous sub-section, we matched our theoretical results for the thermal conductivity at room temperature with the experimentally reported results for the two samples utilizing the parameters given in table 1. Having done that, we extended conductivity calculations for the two samples at several temperatures, below and above room temperature. The results are presented in figure 3.

The difference in the thermal conductivity of the two samples at 10 K is about 163%. This difference is due to difference in the 'effective' grain boundary length which, as mentioned earlier, is due to the addition of Y_2O_3. As noted in the previous sub-section, the change in the density has no effect on the thermal conductivity at low temperatures. In the intermediate temperature range (100–500 K), the increase in the thermal conductivity is due to mixed effects of reduction

in the impurity scattering, reduction in the grain boundary scattering and increase in density. However, the reduction in the impurity scattering is the most influential factor. This reduction is caused by the reaction of Y_2O_3 with the sample, resulting in removal of oxygen impurities from the grains and the formation of the grain boundary phase. The increase in the room-temperature thermal conductivity due to the addition of Y_2O_3 is about 105%. Only 1.7% of this increase is due to the small increase (4.4%) in density. The maximum increase in the conductivity occurs in the intermediate temperature range and can be controlled significantly by using additives.

At temperatures higher than 500 K, the role of phonon–phonon scatterings becomes progressively more important, with phonon–defect scattering becoming less significant. Above the Debye temperature, i.e. above 1200 K, the phonon–phonon scattering is expected to make the dominant contribution towards the conductivity of single crystal AlN. Similarly, at suitably higher temperatures, the conductivity of the AlN ceramic samples should also be dominated by phonon–phonon scattering, and thus increase linearly with increase in the material density. However, our work predicts that between 500 and 2000 K the increase in the conductivity of the ceramic samples only weakly increases with the increase in the material density, and that the phonon–defect scattering is still quite dominant. For example, the 4.4% increase in the density due to sintering with 4 wt% of yttria contributes about 2.6% of the total increase in the thermal conductivity at 1000 K and about 3% at 2000 K. The overall increase in the high temperature conductivity is still considerable, being about 90% at 1000 K (compared to 105% at room temperature).

4. Summary and conclusion

Enhancement in the thermal conductivity of AlN ceramic samples prepared from the application of two nanoscale processing techniques has been investigated theoretically. This has been achieved by including a detailed account of relevant phonon scattering processes and employing the full form of Callaway's conductivity theory. Initially, material and scattering parameters were fitted to reproduce the room-temperature measurements of the conductivity of the samples (microcrystalline AlN with additives and with/without nanoparticle dopants, and nanocrystalline AlN with/without additives). Using these parameters, theoretical predictions have been made for the conductivity over a large temperature range.

The effect of adding nanoparticle dopants to the microcrystalline AlN sample with additives enhances the conductivity by 100%, 155% and 88% at low, room and high temperatures, respectively. On the other hand, the inclusion of additives in the nanocrystalline AlN sample enhances the conductivity by 163%, 105% and 90% at low, room and high temperatures, respectively. In the technologically important intermediate temperature range, the better enhancement in the conductivity of the microcrystalline sample is due to a much higher increase in the densification upon the addition of nanoparticle dopants. The results from this work also show that an increase in material density results in only small 'direct' enhancement in the conductivity (namely due only to the consideration of phonon–phonon interactions). Essentially, densification is a vitally important factor to facilitate and enhance the role played by additives which, in turn, leads to higher thermal conductivity.

Acknowledgment

A AlShaikhi gratefully acknowledges financial support from King Abdulaziz University, Saudi Arabia.

References

[1] Slack G A 1973 *J. Phys. Chem. Solids* **34** 321–35
[2] Werdecker W and Aldinger F 1984 *IEEE Trans. Comp. Hybrids Manuf. Technol.* **7** 399–404
[3] Sheppard L M 1990 *Am. Ceram. Bull.* **69** 1801–3
[4] Kurokawa Y, Utsumi K, Takamizawa H, Kamata T and Noguchi S 1985 *IEEE Trans. Compon. Hybrids Manuf. Technol.* **8** 247–52
[5] Slack G A, Tanzilli R A, Pohl R O and Vandersande J W 1987 *J. Phys. Chem. Solids* **48** 641–7
[6] Watari K, Nakano H, Urabe K, Ishizaki K, Cao S and Mori K 2002 *J. Mater. Res.* **17** 2940–4
[7] Júnior A F and Shanafield D J 2004 *Cerâmica* **50** 247–53
[8] Lee R-R 1991 *J. Am. Ceram. Soc.* **74** 2242–9
[9] Kurokawa Y, Utsumi K and Takamizawa H 1988 *J. Am. Ceram. Soc.* **71** 588–94
[10] Jackson T B, Virkar A V, More K L, Dinwiddie R B and Cutler R A 1997 *J. Am. Ceram. Soc.* **80** 1421–35
[11] Shirakami T, Urabe K and Nakano H 2001 *J. Am. Ceram. Soc.* **84** 631–5
[12] Hsieh C-Y, Lin C-N, Chung S-L, Cheng J and Agrawal D K 2007 *J. Eur. Ceram. Soc.* **27** 343–50
[13] Qiu J, Hotta Y, Watari K and Mitsuishi K 2006 *J. Am. Ceram. Soc.* **89** 377–80
[14] Panchula M L and Ying J Y 2003 *J. Am. Ceram. Soc.* **86** 1121–7
[15] Callaway J 1959 *Phys. Rev.* **113** 1046–51
[16] Srivastava G P 1990 *The Physics of Phonons* (Bristol: Hilger)
[17] Srivastava G P 1976 *Phil. Mag.* **34** 795–809
[18] Srivastava G P 1980 *J. Phys. Chem. Solids* **41** 357–68
[19] Barman S and Srivastava G P 2006 *Phys. Rev.* B **73** 73301–4
[20] Youngman R A and Harris J H 1990 *J. Am. Ceram. Soc.* **73** 3238–46
[21] Klemens P G 1955 *Proc. Phys. Soc.* A **68** 1113 1046–51
[22] Bruls R J, Hintzen H T, de With G, Metselaar R and van Miltenburg J C 2001 *J. Phys. Chem. Solids* **62** 783–92
[23] AlShaikhi A and Srivastava G P 2008 *J. Appl. Phys.* **103** 83554